Shaping Compliance: Inducing Haptic Illusion of Compliance in Different Shapes with Electrotactile Grains

Arata Jingu
HCI Lab
Saarland University,
Saarland Informatics Campus
Saarbrücken, Germany
jingu@cs.uni-saarland.de

Nihar Sabnis
Sensorimotor Interaction
Max Planck Institute for Informatics,
Saarland Informatics Campus
Saarbrücken, Germany
nsabnis@mpi-inf.mpg.de

Paul Strohmeier
Sensorimotor Interaction
Max Planck Institute for Informatics,
Saarland Informatics Campus
Saarbrücken, Germany
paul.strohmeier@mpi-inf.mpg.de

Jürgen Steimle
HCI Lab
Saarland University,
Saarland Informatics Campus
Saarbrücken, Germany
steimle@cs.uni-saarland.de

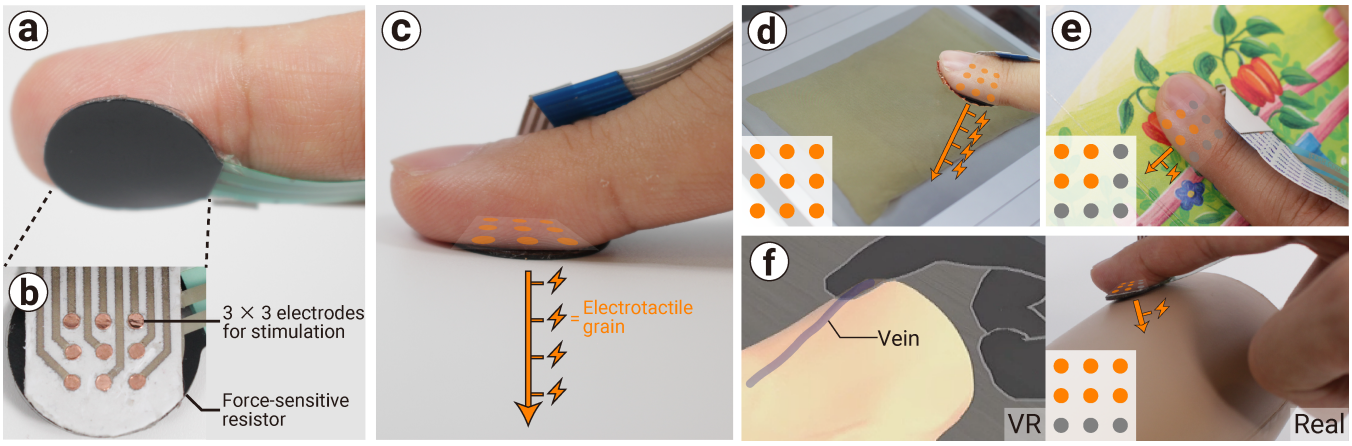

Figure 1: We propose a grain-based electrotactile compliance illusion that makes a rigid surface feel more compliant when pressed. Using (a) a thin and flexible finger-worn interface, (b) comprising a 3 × 3 electrode array and a force-sensitive resistor, (c) the illusion renders compliance by generating a set of short pulses (e.g., electrotactile grain) in response to finger force changes. This electrotactile approach enables rendering compliance of virtual objects *in specific shapes* in a *mobile* form factor for (d) touch screens, (e) physical illustrations, and (f) virtual reality.

ABSTRACT

Compliance, the degree of displacement under applied force, is pivotal in determining the material perception when touching an object. Vibrotactile actuators can be used for creating grain-based virtual compliance, but they have poor spatial resolution and a limiting rigid form factor. We propose a novel electrotactile compliance illusion that renders grains of electrical pulses on an electrode array in response to finger force changes. We demonstrate its ability to render compliance in distinct shapes through a thin, lightweight, and flexible finger-worn interface. Detailed technical parameters and the implementation of our device are provided. A controlled experiment confirms the technique can (1) create virtual compliance; (2) adjust the compliance magnitude with grain and electrode parameters; and (3) render compliance with specific shapes. In three example applications, we present how this illusion can enhance physical objects, elements in graphical user interfaces, and virtual reality experiences.

CHI '24, May 11–16, 2024, Honolulu, HI, USA

ACM ISBN 979-8-4007-0330-0/24/05
https://doi.org/10.1145/3613904.3641907

CCS CONCEPTS

• **Human-centered computing → Haptic devices**.

KEYWORDS

Haptics; haptic illusion; compliance; electrotactile; virtual reality.

ACM Reference Format:
Arata Jingu, Nihar Sabnis, Paul Strohmeier, and Jürgen Steimle. 2024. Shaping Compliance: Inducing Haptic Illusion of Compliance in Different Shapes with Electrotactile Grains. In *Proceedings of the CHI Conference on Human Factors in Computing Systems (CHI '24), May 11–16, 2024, Honolulu, HI, USA.* ACM, New York, NY, USA, 13 pages. https://doi.org/10.1145/3613904.3641907

1 INTRODUCTION

Haptic information of an object is essential for users to capture the object's features that are not conveyed by visual information alone [11]. Compliance, the degree of displacement under applied force [4], is especially pivotal in determining the material perception (e.g., elasticity, softness, depth of displacement) when touching an object [4, 64]. Therefore, reproducing compliance greatly helps users experience the materiality of virtual objects, for instance in virtual reality or on graphical touch screens. It can also help augment or modify the perceived materiality of physical objects, contributing to a growing area of tactile augmented reality. Researchers have presented various approaches for rendering compliance with artificial haptic cues, including kinesthetic cues [64], tactile cues [49], and pseudo-haptics [54]. The grain-based vibrotactile compliance illusion [37] is a widely used approach that renders compliance by generating a short mechanical vibration (called a grain) in response to changes in force. This illusion stems from the observation that vibration is generated when a real object compresses under force, and it can be a useful haptic cue to make a user obtain a sense of pressing a compliant object [37]. Grain-based virtual compliance is one of the most promising approaches because it can express various compliant materials with adjustable parameters [37, 69] and requires only a simple interface comprising an off-the-shelf vibrotactile actuator and a force sensor.

Despite its high potential, vibrotactile stimulation has two major limitations in rendering compliance: Firstly, the spatial resolution in tactile stimuli is low, as it is hard to localize vibration. Therefore, vibrotactile approaches have always rendered compliance on an entire object or surface, rather than providing localized cues. This is a critical issue in reproducing compliance, considering real-world compliant objects have various sizes and shapes, and the user touches them with different areas of the finger pad. Secondly, due to the mechanical actuation involved, vibrotactile actuators are typically rigid and rather bulky. This challenges their integration into body-worn or epidermal devices of advanced form factors and, more generally, into very thin or deformable objects.

To tackle these issues, we propose a novel **grain-based electrotactile compliance illusion**. Inspired by the classical grain-based vibrotactile compliance illusion [37], it creates the illusion of a compliant surface when a rigid surface is pressed, by generating a set of electrical pulses (we call this an electrotactile grain) in response to the force changes. In contrast to the vibrotactile compliance illusion, it uses a fundamentally different form of tactile stimulation, passing a small amount of current from electrodes in contact with the skin to directly stimulate subdermal sensory nerves [30]. Our electrotactile approach not only enables rendering holistic compliance on the entire interface, but it leverages the localized sensation of electrotactile stimuli to also render compliance in a set of basic shapes, such as large or small squares, horizontal or vertical lines. In addition, the electrotactile interface can be realized in a thin and flexible form factor, by printing with conductive ink [76]. Another advantage of electrotactile stimulation compared with vibrotactile stimulation is that electrotactile stimulation has considerably lower energy consumption [82] and is silent.

This paper first introduces the principle underlying the electrotactile illusion and establishes the design space of stimulation parameters (grain, pulse, electrode) for creating the illusion. To achieve it in actual use cases, we have fabricated a 770 µm thin and flexible finger-worn device that combines a 3×3 electrode array with a force-sensitive resistor (FSR). The electrodes and sensor are connected to a standalone low-latency control circuit, which triggers the electrotactile actuation based on the changes in force. We present detailed technical stimulation parameters and the implementation of the device.

Results from a user study confirmed three fundamental findings of grain-based electrotactile compliance illusion: our approach can (1) create virtual compliance; (2) adjust the magnitude of perceived compliance with at least 4 grain levels and 4 electrode conditions; and (3) render compliance with 5 different shapes (large/small squares, horizontal/vertical lines, triangle). Furthermore, based on qualitative feedback from participants, we discuss qualitative aspects of the sensation elicited by the electrotactile illusion.

In three applications, we demonstrate how this approach can produce virtual compliance with shapes for interaction in augmented and virtual reality and in graphical user interfaces. Our examples (1) augment physical objects with virtual compliance, e.g., illustrations in a book, (2) render compliance of graphical elements during interaction on a touch screen, e.g., items on a shopping website, and (3) render the compliance of visual objects in virtual reality environments, e.g., to help dermatology students experience a feel of different skin softness in VR simulation.

In summary, this paper makes the following contributions:

(1) A novel grain-based electrotactile compliance illusion for rendering compliance in adjustable shapes, through a thin, lightweight, and flexible finger-worn interface.
(2) A technical design space of stimulation parameters (grain, pulse, electrode) for creating the illusion and empirical validation of the effects of parameters: adjustability of the compliance magnitude, perceived shapes, and qualitative description of the elicited sensation.
(3) Demonstration of the illusion in example applications that enhance interactions on physical objects, on touch screens, and in virtual reality.

2 RELATED WORK

Our work builds on prior research on rendering compliance, notably the grain-based vibrotactile compliance illusion, as well as prior work on electrotactile interfaces.

2.1 Approaches to Compliance Rendering

Virtual compliance of an object is affected by both kinesthetic and tactile cues generated when the user presses it [4, 37, 64]. Various approaches have explored to artificially reproduce compliance by modulating kinesthetic or tactile cues when the user touches the object. Kinesthetic cues have been used to provide virtual compliance by actually shifting the surface of the mechanical device in

response to the applied force, such as spring mechanisms [62, 64], moving cylinders [6, 17], pneumatic display [65], tilting plates [80], or servo motors [9]. While these approaches pioneered research on virtual compliance, they required bulky mechanical devices to create actual displacement.

Another approach is to render compliance by using tactile cues due to its predominance in compliance perception [64]. Some researchers have explored rendering compliance with tactile cues, such as vibrations [10, 49, 50, 52, 84], skin-stretching [56], electroosmotic pumps [61], or pressure modulation [5, 8, 13–15, 58, 60]. While somewhat smaller, the mechanical components attached to the finger are still rigid. Marchal et al. [45] and Matsubayashi et al. [46] rendered compliance with ultrasound haptics. While the hand was freed from a device, it requires the user to keep their hand in a fixed orientation above grounded ultrasonic transducers, limiting the user's movement and mobility.

Other approaches adopted pseudo-haptics [55] to present virtual compliance with other stimulus modalities, such as visual [1, 10, 23, 54, 84] and auditory [2, 7] stimuli. However, these require constant visual or auditory attention, which can be prohibitive in certain real-world and virtual reality experiences. Another approach, presented by Tao et al. [74], creates a softness sensation by restricting finger pad deformation with a squeezing hollow frame. While this work pioneered altering the compliance of physical objects with a fingerpad-free haptic device, their demonstrated version alters the perceived softness of real-world objects smaller than the fingerpad (e.g., small protrusions), rather than rendering compliance in different shapes on a single surface.

2.2 Grain-Based Vibrotactile Compliance Illusion

One promising method to render compliance is the grain-based vibrotactile compliance illusion [37]. The underlying principle for this method is to provide short mechanical vibrations (called a *grain*) in response to changes in forces applied by the user. The range of sensor output is divided into discrete bins; when the level of force moves into a different bin, a vibrotactile grain is triggered. These grains make the user feel the sensation of pressing a compliant object. This approach can expressively adjust virtual compliance (e.g., elasticity, depth, roughness) [37, 69] with off-the-shelf vibrotactile actuators and force sensors. Due to its simple mechanism, this illusion has been applied to reproduce various haptic sensations, including pressing [39–41], squeezing [38, 42], bending [22, 68], tangential movement [21], and material augmentation [57, 69, 77]. This approach has many control parameters regarding how to make a vibrotactile grain (amplitude, frequency, waveform, duration, etc.) and how to distribute grains on the entire sensor range (the number of grains, the function of grain distribution). In particular, it was shown that the number of grains strongly affects the magnitude and quality (e.g., depth, continuity of cues) of perceived compliance [69]. Furthermore, the function of grain distribution affects the detailed material perception (e.g., softness, naturalness) of virtual compliance. While this grain-based vibrotactile compliance illusion has contributed to presenting expressive virtual compliance with a relatively small device, commonly used vibrotactile actuators are still rather large and thick for direct touch interactions with fingers and incapable of rendering localized and distinct shapes.

2.3 Electrotactile Stimulation

Electrotactile stimulation elicits tactile sensation by applying a small amount of electrical current through skin-exposed electrodes, which directly activates sensory nerves [30]. The current flows from anode electrodes (high voltage) to cathode electrodes (ground). Kajimoto et al. proposed selectively stimulating three mechanoreceptors related to different tactile sensations: Merkel cell disks (SA1) for pressure, Meissner corpuscles (RA) for low-frequency vibration, and Pacinian corpuscles (PC) for high-frequency vibration [32]. Two main modes of stimulation exist: in anodic stimulation, the target electrode is the anode and other electrodes are cathodes; it stimulates RA and elicits an "acute vibratory" sensation. In contrast, in cathodic stimulation, the target electrode is the cathode and all other electrodes are anodes; it stimulates SA1/PC and elicits a "vague pressure" sensation [32, 33]. By stimulating multiple electrodes in order at short time intervals (several tens or hundreds of μs) through high-speed time-division scanning [33, 59], the user can feel a two-dimensional tactile distribution at once. Electrotactile electrodes can be made thin and flexible by printing conductive paths on various substrates, including temporary tattoo paper [76], coated paper [18, 25, 26, 35], flexible printed circuits [47, 75], and silicone [79].

Some works have attempted to render compliance using electrotactile stimulation. Takei et al. [72] presented a softness sensation with a combination of an electrode array and a pressure distribution sensor, by spreading the stimulation area as the user pressed the surface harder. This "area-based" approach is based on the principle that the contact area between the finger pad and an object becomes larger when pressing a softer surface [64]. Similar area-based approaches were taken by [70, 71]. While these area-based approaches opened up the compliance feedback with electrotactile stimulation, they can only express a single compliant surface larger than the finger pad that spreads as the finger presses, not for rendering distinct shapes smaller than the finger pad. Other work has virtual compliance by complimenting electrotactile stimulation to other stimulus modalities, such as vibrotactile stimulation [83], force feedback [70], and visual stimulation [81, 85]. Inspired by these prior works, our work further advances to rendering compliance with *various shapes* via *only* electrotactile stimulation.

3 GRAIN-BASED ELECTROTACTILE COMPLIANCE ILLUSION

In this section, we describe the principle and the stimulation parameters.

3.1 Basic Principle

Inspired by the grain-based vibrotactile compliance illusion, our approach presents virtual compliance by generating a set of electrical pulses–which we call an **electrotactile grain**–in response to changes in the force applied by the user while touching an object or a surface (Figure 2a). The available range of an FSR is divided into discrete bins. An electrotactile grain is triggered when the force value moves into a different bin. For example, as shown in

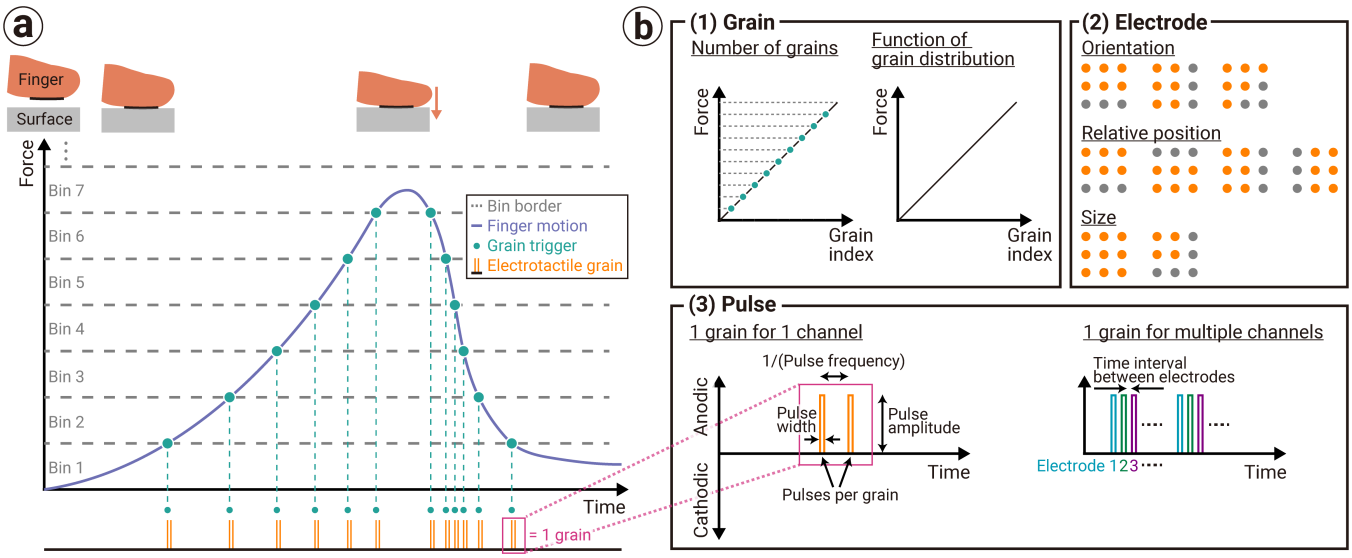

Figure 2: The overview of grain-based electrotactile compliance illusion. (a) The FSR range is divided into discrete bins. An electrotactile grain composed of electrical pulses is generated when the force value moves into a different bin. (b) Our approach has three main parameters: grain, pulse, and electrode.

Figure 2a, an electrotactile grain (composed of two electrical pulses in this example) is triggered when the force value that was in the range of Bin 1 moves into the range of Bin 2. Similar to vibrotactile grains, these simple electrotactile grains work as haptic cues to make the user obtain a sense of pressing a compliant object, as shown later in our evaluation. In contrast to vibrotactile grains, which use vibration, our electrotactile grain uses discrete electrical pulses. This is because, in electrotactile stimulation, the tactile sensation is elicited by discrete electrical pulses. We avoided constant stimulation (i.e., keep generating electrical pulses while pressing the surface regardless of the user's motion) as it has been shown to cause dissociation between the haptic stimuli and the user's action while pressing into an object [57].

It is worth noting that this principle generalizes to many form factors that use an electrotactile interface to stimulate the finger pad and sense force with a synchronized sensor. For instance, implementations could include grounded electrotactile displays, a touchscreen with an electrotactile stimulation layer, or wearable devices. In our implementation, we opted for a thin and flexible device, which can be used as a skin-worn device or attached to the surface of a physical object.

3.2 Stimulation Parameters

Grain-based electrotactile compliance illusion has three main stimulation parameters to control, as depicted in Figure 2b. We will now detail these parameters and provide recommendations on how to adjust them to create a convincing compliance illusion.

Grain parameters. *The number of grains* determines how many grains are triggered when traveling across the full force range, i.e., (number of grains) = (number of bins) - 1. The number of grains affects the magnitude and quality of virtual compliance [69]. As we will empirically show below, the number of grains affects the perceived magnitude of compliance, with more grains creating the perception of high compliance. However, too many grains can induce an unnatural sensation [69] and sensory adaptation of mechanoreceptors [51]. We did not trigger a new grain while a previous one was still being delivered for the same reasons; this is relevant for edge cases of very rapid changes in force. Based on our exploration, we recommend using between 9 and 39 grains, equivalent to 10–40 bins. For example, 9 grains (10 bins) are used in Figure 2b-1 (left). A *function of grain distribution* determines how the grains are distributed to the available force range. It affects the detailed material perception of virtual compliance [69]. This distribution is represented as a function between an index of grains and a force value. For this first investigation and inspired by prior work on vibrotactile grains, we chose a linear distribution, i.e., the grains are evenly distributed across the range of FSR, as shown in Figure 2b-1 (right). Convex and concave functions are other options [37, 69].

Pulse parameters. Electrical pulses in each grain have five parameters: *pulse amplitude*, *pulse frequency*, *pulses per grain*, *pulse polarity*, and *pulse width*. We used a fixed *pulse amplitude* for all grains, as electrotactile stimulation has a narrow range of comfortable intensities between the absolute and pain thresholds [28]. The pulse amplitude was calibrated for each user due to the sensation variability between users [30]. We chose a *pulse frequency* of 125 Hz as it allows the skin to feel stimulation clearly [31] and keeps the grain duration short enough to avoid skipping many grains in case of rapid change of force. Similarly, we used 2 *pulses per grain* to avoid skipping many grains. Regarding *pulse polarity*, we used only anodic pulses because cathodic ones unnaturally caused a tactile sensation at a shifted place from where the finger pressed, as also observed in [30]. We used a *pulse width* of 200 µs to generate a clear and pain-free [30] tactile sensation. We simultaneously stimulated

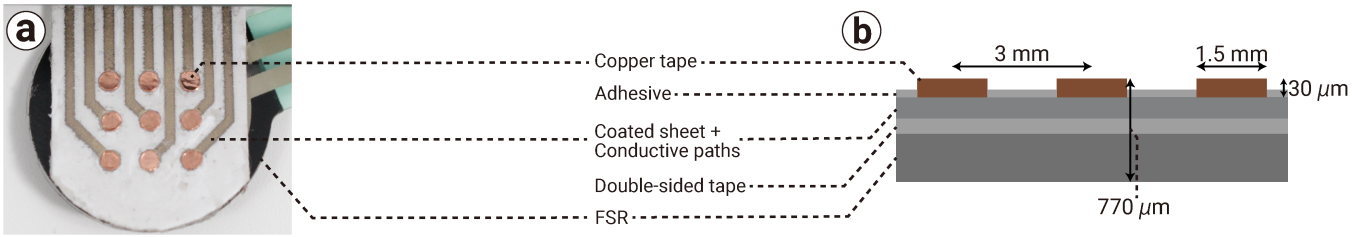

Figure 3: Our finger-worn interface comprises (a) 3 × 3 electrodes and an FSR. (b) They are stacked with double-sided adhesive tape.

multiple electrodes by time-division scanning with a time interval of 50 µs between each electrode to fully discharge electrodes [59].

Electrode parameter. Our electrotactile illusion renders a specific *shape* of virtual compliance by simultaneously stimulating multiple electrodes. In our implementation, we create different shapes with orientations (horizontal, vertical, diagonal), relative positions (top, bottom, left, right), and sizes (large, small). Our pilot study revealed that participants did not feel enough compliance magnitude if only 1–3 electrodes of the interface were active. We therefore created shapes made of 4 or more active electrodes, e.g., squares with 4 or 9 electrodes, lines with 6 electrodes, and triangles with 6 electrodes.

4 IMPLEMENTATION

To achieve this grain-based electrotactile compliance illusion in a wearable form factor, we implemented a finger-worn interface and control circuit.

4.1 Finger-Worn Interface

Our finger-worn interface comprises a printed electrode array and an off-the-shelf FSR, as depicted in Figure 3a. The electrode array has 3 × 3 electrodes of 1.5 mm diameter arranged with 3 mm center-to-center spacing (Figure 3b). This spacing is comparable to the two-point discrimination threshold on the finger pad in electrotactile stimulation (2–4 mm) [33] and is suitable for stimulating Meissner corpuscles with anodic pulses [31]. The electrodes and conductive paths were printed with silver nanoparticle-based ink (Mitsubishi NBSIJ-MU01) on coated paper (Mitsubishi NB-RC-3GR120) using a commodity inkjet printer (EPSON WorkForce WF-2010W). This flexible substrate is robust to loose bending [36]. The electrode array was taped to a flexible flat cable via z-axis conductive tape (3M 9703) and connected to the control circuit. The FSR (Interlink FSR 402) has a linear relationship between applied force and resistance. The sensor value was read through a voltage divider connected to the control circuit.

The printed substrate and the FSR were stacked via double-sided adhesive tape such that the center electrode was placed over the center of the FSR. To ensure close contact between the skin and electrodes, we covered each electrode with a layer of copper tape, cut with a commodity craft cutter (Brother ScanNCut). Finally, we insulated the conductive paths other than electrodes from skin contact by covering them with a laser-cut adhesive sheet. We peeled off its protective sheet before wearing the device and left only adhesive (< 10 µm) to attach the device to the finger. The overall thickness of the interface is 770 µm.

4.2 Control Circuit

We made a custom control circuit based on Teensy 3.5 for generating an electrical current and measuring force value. The current circuit was replicated from [76] and can generate a controlled current in the range of 0–2.7 mA, controllable with 200 discrete steps. It can switch on/off each electrode at 4 kHz (1 period is 250 µs = 200 µs pulse width + 50 µs interval), fast enough for time-division scanning. The current was applied to the desired electrode using two multiplexers (Supertex HV513). The current circuit applied a controlled value of current in a safe range regardless of changes in skin impedance [30, 76]. It therefore constantly measured the current flowing through the skin via a unity-gain voltage differential amplifier (Texas Instruments INA149). The raw FSR value was processed with a low-pass filter to smooth the data [69].

Once provided with stimulation parameters, the control circuit can work stand-alone in generating electrotactile grains in response to changes in force. This is to ensure a very low latency (< 25ms) between the sensor input and electrotactile output, to render convincing grain-based compliance illusions [57]. Stimulation parameters can be initially provided and updated in real-time using either an interface implemented in Python or a Unity interface, both running on a laptop PC (Alienware m17 R5, MacBook Pro 12.6). The control circuit and PC can be connected via Bluetooth or a USB cable (serial port).

5 EVALUATION

To empirically validate the grain-based electrotactile compliance illusion, we conducted a user study consisting of two tasks, investigating (1) the effect of stimulation parameters on the magnitude of the induced compliance and (2) the effect that users can perceive virtual compliance with specific shapes. We also collected qualitative feedback on the elicited sensation. In line with prior work [16, 20, 37, 69], we empirically evaluated the users' subjective experience, as this has proven to be an effective method to investigate "what the haptic experience feels like", which is difficult to capture with other evaluation methods, such as technical evaluations or studies of task performance [67].

We recruited 12 participants (aged 23 to 30; 6 identified as male, 6 as female; 10 right-handed, 2 left-handed). The study took approx. 1.5 hours. This study was approved by the Ethical Review Board of our university (No. 22-11-1).

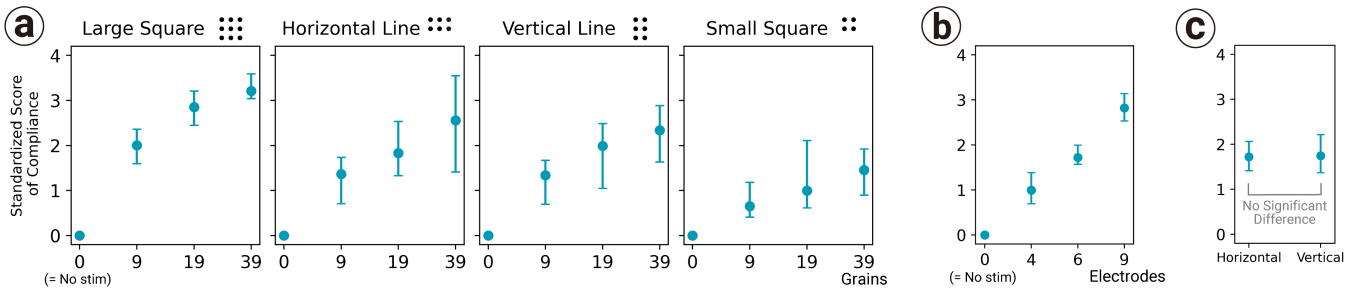

Figure 4: Task 1 investigated the effect of the grain and electrode parameters on the magnitude of perceived compliance. We found (a) a significant difference between all grain levels in each electrode condition, (b) a significant difference between all the electrode conditions, and (c) no significant difference in the orientation of the line shape.

5.1 Task 1: Effect of Stimulation Parameters on Magnitude of Induced Compliance

Our first task aimed to (1) demonstrate that grain-based electrotactile stimulation can induce virtual compliance and (2) investigate the effect of two parameters (grain and electrode) on compliance magnitude. They are fundamental to demonstrating the feasibility and expressiveness of the proposed illusion.

Evaluation method. This task adopted a relative magnitude estimation [24, 66]. This method is well-established as an empirical evaluation in haptics research and suitable for understanding the relation between changes in a physical stimulus and the associated sensation [27]. Thus, it has been used to examine the relation between stimulation parameters and the elicited virtual compliance in prior work [16, 20, 69]. The participant was seated at a desk and pressed the index finger of the dominant hand on the desk's surface. Participants evaluated the relative compliance of the surface while their finger was stimulated, compared to when pressing it without stimuli. This study set a desk as a reference stimulus because our applications require the user to press a hard surface and present a relative virtual compliance compared to its surface. The perceived Shore hardness of the desk through our finger-worn interface was 89A (95A for the desk itself), measured with a durometer (Sauter HBA 100-0, precision ±2A), meaning a *hard* surface [63].

Conditions. We compared the effects of 3 levels of grains (9, 19, 39) and 4 conditions of active electrodes on the virtual compliance, as shown in Figure 4a. The electrode conditions assumed basic shapes when pressing a compliant object with the finger: large square with 3×3 electrodes, small square (2×2), vertical line (2×3), and horizontal line (3×2). The numbers of grains were chosen from our pilot study as they produced different intensities of virtual compliance while avoiding skipping many grains under very rapid changes in applied force.

Study design and procedure. The overall procedure followed past work on relative magnitude estimation [24]. Before the start of the experiment, we explained to the participant the definition of compliance as "the sensation of perceiving that the contact area displaces into the surface under pressure" , and gave specific examples (desk, rubber, polymeric foam). We chose "compliance" because it has a more objective definition compared to a subjective perception of "softness" and therefore can reduce the subjective variation between participants. The participant wore the device on the index finger pad of their dominant hand. In each trial, the participant first experienced the reference condition by pressing the desk surface without electrical stimuli and assumed its compliance to be 0. After the finger was released from the surface, the experimenter turned on a test condition and asked participants to slowly press and release the finger on the surface again. Then, the participant rated the magnitude of perceived virtual compliance of the currently stimulated area. They answered positive values when the test condition was more compliant than the reference, negative values when less compliant, and 0 when they experienced the same compliance. They could freely choose the range and type of numbers for rating (e.g., whole numbers, decimals). They were instructed to map the score only to perceived compliance, not the electrical stimulation intensity or the size of the stimulated area.

The participant continued each trial until they had a clear answer, and could try the reference or test conditions as many times as they wanted. Each participant performed 36 trials (3 grain levels $\times$ 4 electrode conditions $\times$ 3 repetitions). In each repetition, 12 trials were performed in a different counterbalanced order. A short break was followed after each repetition to increase the participant's concentration and alleviate adaptation to electrical stimulation [51]. They were asked to use a consistent scale per repetition.

Calibration. We calibrated the pulse amplitudes before starting each repetition for every participant. Each of the 9 channels was calibrated separately in order due to the variability of tactile sensitivity between skin points [30]. For each channel, the amplitude of a 200ms long stimulus was gradually increased from a minimum value of 0.8 mA and set to a value at which the participant perceived a clear, pain-free stimulus. Finally, we made the participant press the desk surface with the stimulation parameters where the finger was most frequently stimulated (39 grains, all electrodes), and adjusted pulse amplitudes so that the participant felt a pain-free and uniform tactile sensation on the whole stimulated area. We did not ask about virtual compliance at this point. The average amplitude value was 1.59 mA (SD = 0.27).

Results. Figure 4 shows the median and 95 % confidence intervals (CI) of the perceived compliance for all the grain levels and all the electrode conditions. Raw scores were first standardized by dividing by the standard deviation for each participant and each repetition, to reduce variation between participants' scales [69]. Since the data distribution violated normality according to the

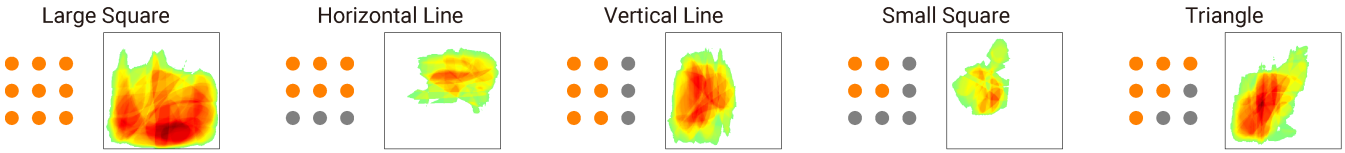

Figure 5: Task 2 confirmed our approach could render compliance with specific shapes. Participants draw the contour of the compliance rendering's shape they perceived. The heatmaps visualize the overlaid normalized contours above a threshold value (128 in 256 levels), drawn for corresponding active electrodes.

Shapiro-Wilk test, we applied Aligned Rank Transform ANOVA (ART ANOVA) for repeated measures [78] for the non-parametric analysis, followed by a post-hoc comparison with the ART-C procedure [12]. We manually added reference conditions (= no stimuli, score = 0) to the raw data in the analysis to confirm the effect of our illusion against the reference.

Figure 4a shows score distributions for each grain level in each electrode condition, together with the reference condition (= no stimuli, 0 grains). ART ANOVA for the two factors (grains and electrode) found a significant difference in both factors ($p < .001$) and found an interaction effect between them ($p < .001$). A post-hoc comparison for the grain level found a significant difference between all grain levels ($p < .01$). This result indicated that a larger number of grains results in a more pronounced perception of compliance. It also indicated that the participants clearly felt higher compliance in all the test conditions than in the reference condition.

In a follow-up analysis, we investigated whether the number of active electrodes affects the magnitude of perceived compliance. Figure 4b shows score distributions for the number of stimulated electrodes (9: large square, 6: horizontal/vertical line, 4: small square), together with the reference condition (= no stimuli, 0 electrodes). ART ANOVA found a significant difference in this condition ($p < .001$). A post-hoc comparison revealed a significant difference between all electrode conditions ($p < .001$). This reveals that using more electrodes for stimulation creates a more pronounced compliance sensation, while already 4 electrodes create a clearly perceivable sensation of compliance. As it is known that tactile perception on the finger pad is not uniform but may depend on the orientation of the stimulus, we specifically compared the two oriented shapes, horizontal vs. vertical line, in a follow-up analysis. Figure 4c shows score distributions for these electrode conditions. ART ANOVA did not find a significant difference between them ($p = .67$).

5.2 Task 2: Shape Perception

Our second task aimed to verify that the proposed approach can make the user perceive virtual compliance with specific shapes.

Conditions. We chose 5 conditions of active electrodes (large square, horizontal line, vertical line, small square, triangle), adding another distinct shape of the triangle to the other basic shapes, as shown in Figure 5. We used 39 grains for all the electrode conditions.

Trial design and procedure. Participants wore our device on the index finger pad of their non-dominant hand and held a stylus pen with their dominant hand. Because we assume no difference in tactile sensitivity between the dominant and non-dominant index finger [19], we chose the non-dominant hand for perceiving the tactile stimuli, to keep the user's dexterous dominant hand free for sketching with the stylus. In each trial, the participant experienced a test condition in the same way as in Task 1. We first asked the participant if they felt higher compliance than the reference condition (= no stimuli). Then, for spatial reference, the experimenter showed a piece of paper above the participant's finger with the same shape and size as the stimulation device, indicating the stimulation area with a square. Then, the participant experienced the test condition and was tasked to draw on a tablet the closed contour of the area they felt compliance. They could draw multiple separate contours if needed. Each participant performed 15 trials (5 shapes × 3 repetitions) in a randomized order without a break. We conducted the same calibration as Task 1 before the trials. The average amplitude value was 1.70 mA (SD = 0.28). One trial was felt as less compliant than the reference condition and was removed.

Results. Figure 5 shows heatmaps of the shapes drawn by the participants, separately for each shape. The scale of the raw contours was first normalized between participants to correct for potential bias due to differences in how participants conceptually mapped the stimulated area on the fingerpad to the drawing area on the tablet. Separately for each participant, we aggregated all contours drawn by the participant, calculated the bounding box surrounding them, and calculated a transformation matrix from this bounding box to a square of the normalized size of 340 × 340 pixels, and scaled all the contours with this transformation matrix. Then, aggregating these normalized contours of all the participants, we generated heatmaps with 256 levels (higher is close to red, lower is to blue) with the brightest pixel out of all the heatmaps as the maximum value (255). Figure 5 displays only the areas above a threshold value of the middle level (= 128). For reference, the active electrodes are shown left of each heatmap (orange is active, gray is inactive).

These heatmaps show that the contours roughly matched the area of stimulated electrodes in each shape, indicating that participants were able to localize the part of the fingertip where they felt compliance with a given shape. The results also show that increasing the stimulation area (e.g., large square) resulted in a larger perceived stimulation area. We observe slightly larger offsets between active electrodes and perceived area for the vertical axis than for the horizontal axis—see for instance the top and bottom area of large square. This observation may be attributed to the asymmetric haptic sensitivity of the finger pad depending on direction [3, 34]. The variance between participants can be attributed to the differences in tactile sensitivity on the finger pads.

5.3 Qualitative Feedback

Induced sensation. After Task 1 and 2 were completed, we first asked participants to describe the induced sensation in our study. Participants described similar sensations as uncovered for the grain-based vibrotactile compliance illusion [37]: *"elastic"* (P1), *"bouncy"* (P1), *"squishy"* (P2), *"soft"* (P6), *"can press further"* (P5), *"there's longer distance till I press to the point where I cannot press further"* (P1), or *"like pressing a surface that could displace more if I press harder"* (P7). Interestingly, some participants felt roughness or smoothness of the surface texture of a virtual compliant object: *"a rough area"* (P8), *"[the high-rated trials are] more coarse. (...) [the low-rated ones] are smooth because the intensity is low and I cannot really feel each individual dot (...)"* (P1), and *"[the high-rated trials are] tickling a little bit like touching sponge. [For low-rated ones,] the type of sensation was similar, but usually weaker"* (P10).

Comparing to real-world objects. Next, we asked participants which real-world object was reminded by the induced sensation when they rated it with high or low scores. For high ratings, they answered: *"sponge"* (P3, P7, P9, P10), *"[polymeric] foam"* (P4, P5, P10, P12), *"pillow"* (P1, P2), *"grass"* (P10), or *"popping bubbles"* (P4). P1 added *"I would say something that's not so smooth but has a lot of elasticity and compliance so you can push down"*. For low ratings, they answered: *"clothes"* (P3), *"tree"* (P8), *"book"* (P9), *"eraser"* (P5), or *"the soft material printed by a PolyJet Printer"* (P1). P1 commented *"there's less displacement as I press down, and it makes me feel like I only just like move a little bit. Or not as much until I hit the very flat desk"*. P6, the only participant who answered negative scores for some trials, expressed *"like metal surfaces that are very hard"* for their negative scores because *"there's no way bending it or putting any dent in there. And even harder than the material of the table"*.

Realism. Other than our questions, three participants mentioned the realism of induced compliance. Note that the "magnitude" of compliance (investigated in our study) and its "realism" are different factors. They commented: *"when the intensity is very high, (...) it feels artificial. And when intensity is not low but is a medium level, (...) [it] feels like it's a natural sensation."* (P2), *"[when] I felt the stimulation clearly but it wasn't too strong (...) I was able to think of it as compliance"* (P4) , and *"the lower compliance one feels more like natural materials"* (P1). P2 additionally commented on the lack of congruence between visual and haptic stimuli in our experiment: *"when the sensation feels like only one point [= considered to be the "small square" condition] on my finger, that doesn't feel real. Because when I am pushing the desk, I would expect all my finger [area to feel compliance]"*.

5.4 General Discussion

Task 1 confirmed the grain-based electrotactile compliance illusion. Furthermore, the findings show that the magnitude of the virtual compliance can be adjusted with the number of grains (at least 4 levels: 0, 9, 19, 39 grains) and the number of active electrodes (at least 4 conditions: 0, 4, 6, 9). Compliance was intensified with an increasing number of grains or electrodes used. These findings can be expected because the participants received haptic cues of compliance more frequently (i.e., more grains) and on a larger skin area (i.e., more electrodes). Our findings on the role of the number of electrotactile grains are similar to findings on grain-based vibrotactile compliance illusions, which found that compliance could be felt most clearly with stimuli spanning between 13 and 53 grains [69].

Findings from Task 2 indicate the proposed illusion can render compliance with specific shapes. Our study participants were able to draw quite accurate contours despite the demanding nature of this task. The task was challenging because (1) the electrode spacing (3 mm) is just as small as the electrotactile two-point discrimination threshold; (2) electrotactile stimulation has a large variability of the sensation between persons or stimulated points [30], leading to the high variability in a task to draw the perceived stimulated area [73]; and (3) participants had to convert the perception of haptic stimuli to visual contours. The relatively larger shifts in the vertical axis may be attributed to the asymmetric haptic sensitivity of the finger pad depending on the direction [3, 34]. This is reflected in P1's comment on Task 2: *"I can tell if it's really different, like left or right, but then in the vertical axis, I cannot tell how much of a difference"*.

Qualitative feedback from participants clarified what type of stimulus our approach is best suited to express. Participants tended to relate the high-rated conditions in Task 1 to a more compliant object with a rougher surface, and the low-rated ones to a less compliant object with a smoother surface. It is reasonable because the high-rated conditions (i.e., more frequent haptic cues with more electrodes) emphasize the acute sensation of electrical stimuli more, and vice versa. Note that here, rough and smooth refer to the 2D surface texture of a compliant object, rather than the texture sensation felt when pressing the surface along the z-axis (i.e., regularity of the displacement movement) [37]. This rough texture sensation is attributed to anodic stimulation [33] and quite different from the vibrotactile illusion that produces the sensation of a smooth surface texture regardless of the compliance magnitude [37]. In future work, we might be able to render various surface textures by adjusting the pulse parameters or instead even use cathodic stimulation to create a smooth texture with high compliance, although the latter might be incapable of rendering distinct shapes.

Another key perspective is the importance of congruence between visual and haptic stimuli. Some participants found unnaturalness when experiencing virtual compliance with shapes or a rough texture on the desk. It motivated us to present visual stimuli matching the shape and the texture of rendered compliance in our following applications.

6 APPLICATIONS

This section demonstrates how our approach augments three interfaces with virtual compliance: (1) physical real-world objects, (2) graphical user interfaces on touch screens, and (3) virtual reality. We believe these interfaces can become even more informative and expressive by rendering the compliance of otherwise visual-only content.

6.1 Augmenting Physical Objects with Virtual Compliance

Paper has traditionally been used for conveying visual information effectively, such as picture books, textbooks at school, artworks, or advertisements. Our approach further enables existing paper illustrations to be augmented with virtual compliance. Figure 6

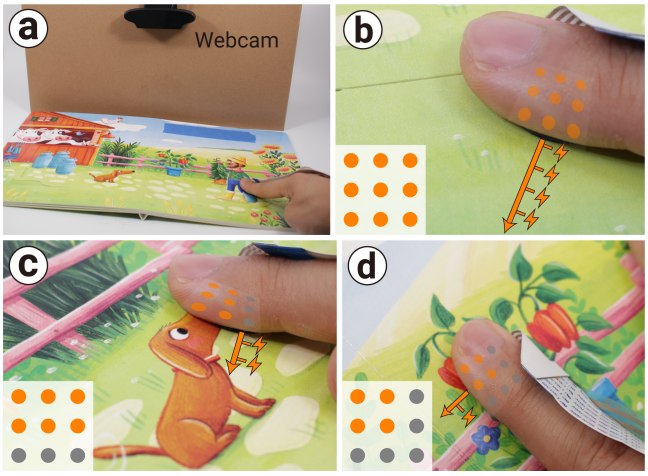

Figure 6: (a) Our approach renders compliance when the user reads a picture book and touches an illustration: (b) a large area of soft grass underneath the entire fingerpad, (c) a squishy horizontally-shaped dog nose, and (d) an unripe and hard vegetable that is small.

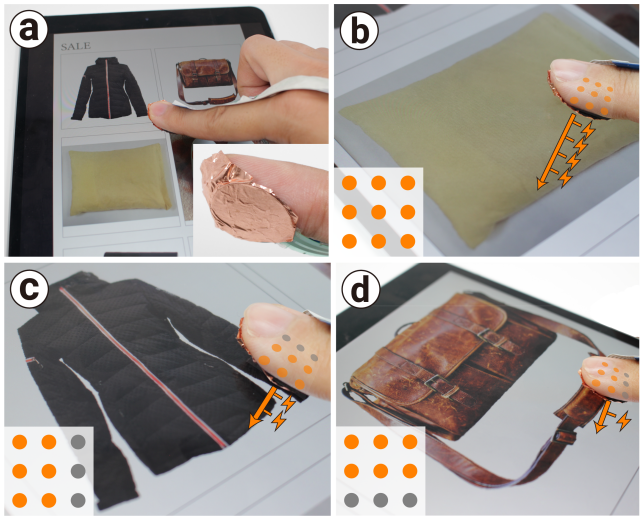

Figure 7: (a) Our approach renders compliance when the user touches an item of an online shopping website on a touch screen: (b) a large fluffy cushion, (c) an elastic vertical sleeve of a jacket, and (d) a horizontal stiff strap of a bag.

depicts a user reading a picture book made of stiff paper. (a) The camera above the book is connected to a MacBook. It tracks the position of the index finger by processing images with Python and Google MediaPipe, and sends the position information to our control circuit via a USB cable to reduce latency. When the user presses an illustration, our device renders appropriate compliance for the touched visual element, such as (b) soft grass (39 grains, large square), (c) a squishy dog nose (19 grains, horizontal line), and (d) an unripe and hard vegetable (9 grains, small square). The stimulation parameters of applications are set according to the outcomes of the user study.

6.2 Rendering Compliance for Interactions on a Touch Screen

Capacitive touch screens allow users to manipulate visual information intuitively with their fingers and are pervasive in smartphones, tablets, and smartwatches. Our approach further adds virtual compliance to these visual displays while the user operates the touch screen with their fingers. Figure 7 depicts a user browsing an online shopping website with a capacitive touch screen. The touch screen is directly connected to our control circuit via a USB cable and sends the touch position to it. (a) The user scrolls down the screen. The stimulation is turned off at this point. The user finds an item and checks its feel with a finger press. The touch screen detects the touch position and sends the position information to our system. Our device renders compliance corresponding to the touched item, including (b) a fluffy cushion (39 grains, large square), (c) an elastic sleeve of a jacket (19 grains, vertical line), and (d) a slightly stiff strap of a bag (9 grains, horizontal line). To allow the touch screen to detect the finger touch, we slightly modified our device by adding a piece of copper tape onto its outer side and connecting it to the finger, acting as a passive electrode for capacitive coupling between the finger and the touch sensor. We did not observe any electrical interference between capacitive touch sensing and electrical stimulation.

6.3 Rendering the Compliance of Visual Objects in Virtual Reality Experiences

VR can freely reproduce 3D visual information of objects and is an emerging technology in simulations, education, and games. Our interface can complement the compliance of visual objects in VR experiences. For instance, this can be useful in the training for medical staff to find veins or to assess the skin surface conditions (e.g., stiffness, texture, temperature) of a patient through palpation [53]. We implemented a simple application example with Unity on Alienware demonstrating how a VR simulation for medical training could help students learn how to assess the skin surface through finger touch using a 3D printed rigid model of a human arm (Figure 8): (a) The user wears a commercial VR head-mounted display (Meta Quest 2), which tracks the position of the finger and a physical arm model through an ArUco marker. The positions of virtual and physical arm models are aligned. (b) When the user touches a skin area, our device simulates its softness (19 grains, large square). (c) When the user touches a virtual vein, our device simulates its stiffer sensation than the other skin area (9 grains, horizontal line).

7 LIMITATIONS AND FUTURE WORK

In this first work on grain-based electrotactile compliance illusions, we focused on clarifying its fundamental characteristics. Future work should investigate further stimulation parameters more deeply (e.g., the function of grain distribution, polarity, and frequency) as well as the effect of rendering compliance on other body parts (e.g., palm, foot sole). It will also be interesting to combine the proposed method with other existing compliance feedback methods

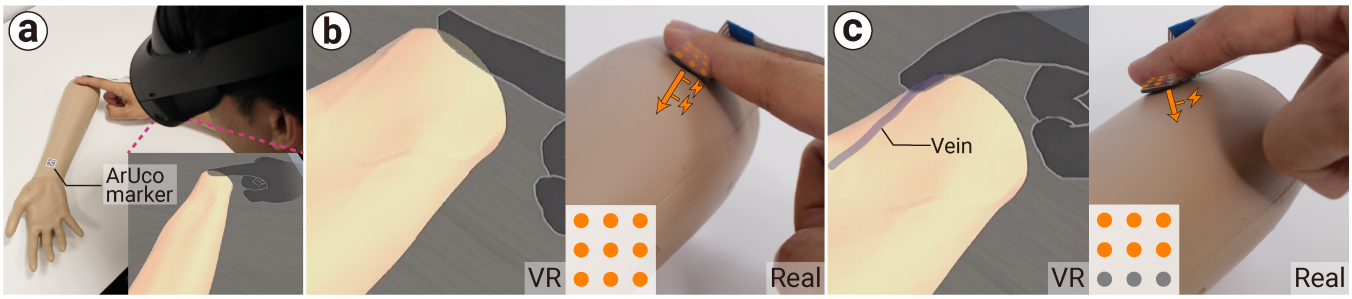

Figure 8: (a) Rendering compliance in a VR medical simulation. When the user touches a physical hand model, our device presents the sensation of (b) soft skin or (c) a thin and stiffer vein.

(e.g., the vibrotactile illusion [37], the area-based approach using electrotactile stimulation [72], or pseudo-haptics [54]) and study application opportunities in more detail. Another relevant question for future work is to compare our proposed illusion to these other compliance feedback methods and investigate more detailed haptic features of rendered compliance (e.g., depth, texture, elasticity, comparison to real-world objects, and realism).

This first study used only a basic finger-worn device combining 9 electrodes with an FSR. However, the proposed illusion is not limited to this form factor. It could also be integrated into physical surfaces or objects, even deformable ones, due to thin and flexible electrodes used in electrotactile stimulation. Ultra-thin and stretchable epidermal interfaces [48] could be achieved by combining a feel-through electrotactile interface [76] with ultra-thin pressure sensors [43]. A further promising avenue is to render more diverse shapes with higher resolution electrode matrices or super-resolution rendering [44].

This paper only investigated rendering compliance when the user presses on a rigid and planar surface. Future work should examine if the grain-based electrotactile compliance illusion works on softer or curved surfaces too, and what absolute hardness values the perceived virtual compliance corresponds to.

Similar to other electrotactile stimulation works, our interface can induce sensation variability for long-term use due to sweat, finger motion, and sensory adaptation [29, 51]. We plan to integrate an impedance measurement circuit to adjust pulse amplitudes in real-time and suppress the sensation variability [18, 29].

Finally, further minimization of the device prototype is an important consideration for practical deployment, comprising wireless communication between the finger-worn interface and a more compact control circuit.

8 CONCLUSION

We proposed a novel grain-based electrotactile compliance illusion that renders compliance by generating an electrical grain of electrical pulses in response to changes in force applied by the finger. It enables rendering compliance with shapes in a thin, lightweight, flexible form factor, which tackles the issues of the conventional vibrotactile illusion: low spatial resolution in tactile stimuli and bulky form factor. We presented a technical design space of stimulation parameters (grain, pulse, electrode) for creating the illusion. To achieve this illusion in a wearable form factor, we fabricated a 770 µm thin and flexible finger-worn device that combines a 3×3 electrode array with an FSR. A controlled experiment confirmed that the proposed illusion could (1) create virtual compliance; (2) adjust the compliance magnitude with grain and electrode parameters; and (3) render compliance in specific shapes. Qualitative feedback from participants clarified what type of stimulus our approach is best suited to express. It also indicated our approach might open up another novel area in rendering compliance: 2D surface texture of a compliant object. In three example applications, we presented how this illusion can enhance the interaction with physical objects, on touch screens, and in virtual reality.

As the grain-based electrotactile compliance illusion is not restricted to the wearable device form factor investigated in this work, we recommend that future work more broadly investigate how this novel illusion can contribute to other forms of haptics interfaces, including electrotactile displays that are grounded or embedded inside objects, and how high-resolution electrode interfaces can render more diverse shapes. We are excited about a future that will deeply and seamlessly integrate the feel of objects into digital media and hope our work contributes a valuable step toward realizing this vision.

ACKNOWLEDGMENTS

This project received funding from the European Research Council under the ERC Proof of Concept grant (ERC POC 101113226). Arata Jingu is a recipient of Funai Overseas Scholarship.

REFERENCES

[1] Oscar Javier Ariza Nunez, André Zenner, Frank Steinicke, Florian Daiber, and Antonio Krüger. 2022. Holitouch: Conveying Holistic Touch Illusions by Combining Pseudo-Haptics With Tactile and Proprioceptive Feedback During Virtual Interaction With 3DUIs. *Frontiers in Virtual Reality* 3 (2022). https://www.frontiersin.org/articles/10.3389/frvir.2022.879845

[2] Federico Avanzini and Paolo Crosato. 2006. Haptic-Auditory Rendering and Perception of Contact Stiffness, Vol. 4129. 24–35. https://doi.org/10.1007/11821731_3

[3] S. J. Bensmaia, S. S. Hsiao, P. V. Denchev, J. H. Killebrew, and J. C. Craig. 2008. The tactile perception of stimulus orientation. *Somatosensory & Motor Research* 25, 1 (Jan. 2008), 49–59. https://doi.org/10.1080/08990220701830662

[4] Wouter M. Bergmann Tiest and Astrid M. L. Kappers. 2009. Cues for Haptic Perception of Compliance. *IEEE Transactions on Haptics* 2, 4 (Oct. 2009), 189–199. https://doi.org/10.1109/TOH.2009.16

[5] Matteo Bianchi and Alessandro Serio. 2015. Design and Characterization of a Fabric-Based Softness Display. *IEEE Transactions on Haptics* 8, 2 (April 2015), 152–163. https://doi.org/10.1109/TOH.2015.2404353

[6] A. Bicchi, E.P. Scilingo, and D. De Rossi. 2000. Haptic Discrimination of Softness in Teleoperation: The Role of the Contact Area Spread Rate. *IEEE Transactions*

on Robotics and Automation 16, 5 (Oct. 2000), 496–504. https://doi.org/10.1109/70.880800

[7] F.J. Canadas-Quesada and A. Reyes-Lecuona. 2006. Improvement of perceived stiffness using auditory stimuli in haptic virtual reality. In *MELECON 2006 - 2006 IEEE Mediterranean Electrotechnical Conference*. 462–465. https://doi.org/10.1109/MELCON.2006.1653138 ISSN: 2158-8481.

[8] Francesco Chinello, Claudio Pacchierotti, Monica Malvezzi, and Domenico Prattichizzo. 2018. A Three Revolute-Revolute-Spherical Wearable Fingertip Cutaneous Device for Stiffness Rendering. *IEEE Transactions on Haptics* 11, 1 (Jan. 2018), 39–50. https://doi.org/10.1109/TOH.2017.2755015

[9] Inrak Choi, Eyal Ofek, Hrvoje Benko, Mike Sinclair, and Christian Holz. 2018. CLAW: A Multifunctional Handheld Haptic Controller for Grasping, Touching, and Triggering in Virtual Reality. In *Proceedings of the 2018 CHI Conference on Human Factors in Computing Systems (CHI '18)*. Association for Computing Machinery, New York, NY, USA, 1–13. https://doi.org/10.1145/3173574.3174228

[10] Inrak Choi, Yiwei Zhao, Eric J. Gonzalez, and Sean Follmer. 2020. Augmenting Perceived Softness of Haptic Proxy Objects Through Transient Vibration and Visuo-Haptic Illusion in Virtual Reality. *IEEE Transactions on Visualization and Computer Graphics* 27, 12 (2020), 4387–4400. https://doi.org/10.1109/TVCG.2020.3002245

[11] Heather Culbertson, Samuel B. Schorr, and A. Okamura. 2018. Haptics: The Present and Future of Artificial Touch Sensation. *Annual Review of Control, Robotics, and Autonomous Systems* (2018). https://doi.org/10.1146/ANNUREV-CONTROL-060117-105043

[12] Lisa A. Elkin, Matthew Kay, James J. Higgins, and Jacob O. Wobbrock. 2021. An Aligned Rank Transform Procedure for Multifactor Contrast Tests. In *The 34th Annual ACM Symposium on User Interface Software and Technology (UIST '21)*. Association for Computing Machinery, New York, NY, USA, 754–768. https://doi.org/10.1145/3472749.3474784

[13] Simone Fani, Simone Ciotti, Edoardo Battaglia, Alessandro Moscatelli, and Matteo Bianchi. 2018. W-FYD: A Wearable Fabric-Based Display for Haptic Multi-Cue Delivery and Tactile Augmented Reality. *IEEE Transactions on Haptics* 11, 2 (April 2018), 304–316. https://doi.org/10.1109/TOH.2017.2708717

[14] Simone Fani, Simone Ciotti, Giulia Pagnanelli, Alessandro Moscatelli, Yuri De Pra, and Matteo Bianchi. 2023. Modulating the Perceived Softness of Real Objects Through Wearable Feel-Through Haptics. *IEEE transactions on haptics* PP (May 2023). https://doi.org/10.1109/TOH.2023.3271825

[15] Gabriele Frediani and Federico Carpi. 2020. Tactile display of softness on fingertip. *Scientific Reports* 10, 1 (Nov. 2020), 20491. https://doi.org/10.1038/s41598-020-77591-0

[16] Robert M. Friedman, Kim D. Hester, Barry G. Green, and Robert H. LaMotte. 2008. Magnitude estimation of softness. *Experimental Brain Research* 191, 2 (Nov. 2008), 133–142. https://doi.org/10.1007/s00221-008-1507-5

[17] Kinya Fujita and Hisayuki Ohmori. 2001. A New Softness Display Interface by Dynamic Fingertip Contact Area Control.

[18] Daniel Groeger, Martin Feick, Anusha Withana, and Jürgen Steimle. 2019. Tactlets: Adding Tactile Feedback to 3D Objects Using Custom Printed Controls. In *Proceedings of the 32nd Annual ACM Symposium on User Interface Software and Technology (UIST '19)*. Association for Computing Machinery, New York, NY, USA, 923–936. https://doi.org/10.1145/3332165.3347937

[19] J. J. Hage, L. P. van der Steen, and P. J. de Groot. 1995. Difference in sensibility between the dominant and nondominant index finger as tested using the Semmes-Weinstein monofilaments pressure aesthesiometer. *The Journal of Hand Surgery* 20, 2 (March 1995), 227–229. https://doi.org/10.1016/s0363-5023(05)80012-7

[20] Joyoung Han and Geehyuk Lee. 2021. Finding a More Pleasant Compliance Illusion Method for a Hand-Held Device. *IEEE Access* 9 (2021), 168154–168161. https://doi.org/10.1109/ACCESS.2021.3137614

[21] Seongkook Heo and Geehyuk Lee. 2017. Vibrotactile Compliance Feedback for Tangential Force Interaction. *IEEE transactions on haptics* 10, 3 (2017), 444–455. https://doi.org/10.1109/TOH.2016.2604305

[22] Seongkook Heo, Jaeyeon Lee, and Daniel Wigdor. 2019. PseudoBend: Producing Haptic Illusions of Stretching, Bending, and Twisting Using Grain Vibrations. In *Proceedings of the 32nd Annual ACM Symposium on User Interface Software and Technology (UIST '19)*. Association for Computing Machinery, New York, NY, USA, 803–813. https://doi.org/10.1145/3332165.3347941

[23] Yuichi Hirano, Asako Kimura, Fumihisa Shibata, and Hideyuki Tamura. 2011. Psychophysical influence of mixed-reality visual stimulation on sense of hardness. *2011 IEEE Virtual Reality Conference* (March 2011), 51–54. https://doi.org/10.1109/VR.2011.5759436

[24] Yu Huang and Michael J. Griffin. 2014. Comparison of absolute magnitude estimation and relative magnitude estimation for judging the subjective intensity of noise and vibration. *Applied Acoustics* 77 (March 2014), 82–88. https://doi.org/10.1016/j.apacoust.2013.10.003

[25] Arata Jingu, Yudai Tanaka, and Pedro Lopes. 2023. LipIO: Enabling Lips as both Input and Output Surface. In *Proceedings of the 2023 CHI Conference on Human Factors in Computing Systems (CHI '23)*. Association for Computing Machinery, New York, NY, USA, 1–14. https://doi.org/10.1145/3544548.3580775

[26] Arata Jingu, Anusha Withana, and Jürgen Steimle. 2023. Double-Sided Tactile Interactions for Grasping in Virtual Reality. In *Proceedings of the 36th Annual ACM Symposium on User Interface Software and Technology (UIST '23)*. Association for Computing Machinery, New York, NY, USA, 1–11. https://doi.org/10.1145/3586183.3606798

[27] Lynette A. Jones and Hong Z. Tan. 2013. Application of Psychophysical Techniques to Haptic Research. *IEEE Transactions on Haptics* 6, 3 (July 2013), 268–284. https://doi.org/10.1109/TOH.2012.74

[28] K.A. Kaczmarek, J.G. Webster, P. Bach-y Rita, and W.J. Tompkins. 1991. Electrotactile and Vibrotactile Displays for Sensory Substitution Systems. *IEEE Transactions on Biomedical Engineering* 38, 1 (Jan. 1991), 1–16. https://doi.org/10.1109/10.68204

[29] Hiroyuki Kajimoto. 2012. Electrotactile Display with Real-Time Impedance Feedback Using Pulse Width Modulation. *IEEE Transactions on Haptics* 5, 2 (April 2012), 184–188. https://doi.org/10.1109/TOH.2011.39

[30] Hiroyuki Kajimoto. 2016. Electro-tactile Display: Principle and Hardware. In *Pervasive Haptics: Science, Design, and Application*, Hiroyuki Kajimoto, Satoshi Saga, and Masashi Konyo (Eds.). Springer Japan, Tokyo, 79–96. https://doi.org/10.1007/978-4-431-55772-2_5

[31] Hiroyuki Kajimoto, N Kawakami, and Susumu Tachi. 2003. Psychophysical evaluation of receptor selectivity in electro-tactile display. *Proceeding of 13th International Symposium on Measurement and Control in Robotics* (Jan. 2003).

[32] Hiroyuki Kajimoto, Naoki Kawakami, and Susumu Tachi. 2004. Electro-Tactile Display with Tactile Primary Color Approach. *Int. Conf. on Intelligent Robots and Systems, 2004* (2004). https://cir.nii.ac.jp/crid/1573387450270742784

[33] H. Kajimoto, N. Kawakami, S. Tachi, and M. Inami. 2004. SmartTouch: electric skin to touch the untouchable. *IEEE Computer Graphics and Applications* 24, 1 (Jan. 2004), 36–43. https://doi.org/10.1109/MCG.2004.1255807

[34] Astrid M L Kappers and Jan J Koenderink. 1999. Haptic Perception of Spatial Relations. *Perception* 28, 6 (June 1999), 781–795. https://doi.org/10.1068/p2930

[35] Kunihiro Kato, H. Ishizuka, H. Kajimoto, and Homei Miyashita. 2018. Double-sided Printed Tactile Display with Electro Stimuli and Electrostatic Forces and its Assessment. *CHI* (2018). https://doi.org/10.1145/3173574.3174024

[36] Yoshihiro Kawahara, Steve Hodges, Nan-Wei Gong, Simon Olberding, and Jürgen Steimle. 2014. Building Functional Prototypes Using Conductive Inkjet Printing. *IEEE Pervasive Computing* 13, 3 (July 2014), 30–38. https://doi.org/10.1109/MPRV.2014.41

[37] Johan Kildal. 2010. 3D-Press: Haptic Illusion of Compliance when Pressing on a Rigid Surface. In *International Conference on Multimodal Interfaces and the Workshop on Machine Learning for Multimodal Interaction (ICMI-MLMI '10)*. Association for Computing Machinery, New York, NY, USA, 1–8. https://doi.org/10.1145/1891903.1891931

[38] Johan Kildal. 2012. Kooboh: Variable Tangible Properties in a Handheld Haptic-Illusion Box. In *Haptics: Perception, Devices, Mobility, and Communication (Lecture Notes in Computer Science)*, Poika Isokoski and Jukka Springare (Eds.). Springer, Berlin, Heidelberg, 191–194. https://doi.org/10.1007/978-3-642-31404-9_33

[39] Hwan Kim, Minhwan Kim, and Woohun Lee. 2016. HapThimble: A Wearable Haptic Device towards Usable Virtual Touch Screen. In *Proceedings of the 2016 CHI Conference on Human Factors in Computing Systems (CHI '16)*. Association for Computing Machinery, New York, NY, USA, 3694–3705. https://doi.org/10.1145/2858036.2858196

[40] Hwan Kim, HyeonBeom Yi, Hyein Lee, and Woohun Lee. 2018. HapCube: A Wearable Tactile Device to Provide Tangential and Normal Pseudo-Force Feedback on a Fingertip. In *Proceedings of the 2018 CHI Conference on Human Factors in Computing Systems (CHI '18)*. Association for Computing Machinery, New York, NY, USA, 1–13. https://doi.org/10.1145/3173574.3174075

[41] Sunjun Kim and Geehyuk Lee. 2013. Haptic Feedback Design for a Virtual Button Along Force-Displacement Curves. In *Proceedings of the 26th annual ACM symposium on User interface software and technology (UIST '13)*. Association for Computing Machinery, New York, NY, USA, 91–96. https://doi.org/10.1145/2501988.2502041

[42] Jaeyeon Lee, Mike Sinclair, Mar Gonzalez-Franco, Eyal Ofek, and Christian Holz. 2019. TORC: A Virtual Reality Controller for In-Hand High-Dexterity Finger Interaction. In *Proceedings of the 2019 CHI Conference on Human Factors in Computing Systems*, Vol. ca. ACM, Glasgow Scotland Uk, 1–13. https://doi.org/10.1145/3290605.3300301

[43] Sunghoon Lee, Sae Franklin, Faezeh Arab Hassani, Tomoyuki Yokota, Md Osman Goni Nayeem, Yan Wang, Raz Leib, Gordon Cheng, David W. Franklin, and Takao Someya. 2020. Nanomesh pressure sensor for monitoring finger manipulation without sensory interference. *Science* 370, 6519 (Nov. 2020), 966–970. https://doi.org/10.1126/science.abc9735

[44] Weikang Lin, Dongsheng Zhang, Wang Wei Lee, Xuelong Li, Ying Hong, Qiqi Pan, Ruirui Zhang, Guoxiang Peng, Hong Z. Tan, Zhengyou Zhang, Lei Wei, and Zhengbao Yang. 2022. Super-resolution wearable electrotactile rendering system. *Science Advances* 8, 36 (Sept. 2022), eabp8738. https://doi.org/10.1126/sciadv.abp8738

[45] M. Marchal, G. Gallagher, A. Lécuyer, and C. Pacchierotti. 2020. Can Stiffness Sensations Be Rendered in Virtual Reality Using Mid-air Ultrasound Haptic Technologies?. In *Haptics: Science, Technology, Applications (Lecture Notes in*

Computer Science), Ilana Nisky, Jess Hartcher-O'Brien, Michaël Wiertlewski, and Jeroen Smeets (Eds.). Springer International Publishing, Cham, 297–306. https://doi.org/10.1007/978-3-030-58147-3_33

[46] Atsushi Matsubayashi, Tomohisa Yamaguchi, Yasutoshi Makino, and Hiroyuki Shinoda. 2021. Rendering Softness Using Airborne Ultrasound. In *2021 IEEE World Haptics Conference (WHC)*. 355–360. https://doi.org/10.1109/WHC49131.2021.9517219

[47] Dinmukhammed Mukashev, Nimesha Ranasinghe, and Aditya Shekhar Nittala. 2023. TactTongue: Prototyping ElectroTactile Stimulations on the Tongue. In *Proceedings of the 36th Annual ACM Symposium on User Interface Software and Technology (UIST '23)*. Association for Computing Machinery, New York, NY, USA, 1–14. https://doi.org/10.1145/3586183.3606829

[48] Aditya Shekhar Nittala and Jürgen Steimle. 2022. Next Steps in Epidermal Computing: Opportunities and Challenges for Soft On-Skin Devices. In *CHI Conference on Human Factors in Computing Systems (CHI '22)*. Association for Computing Machinery, New York, NY, USA, 1–22. https://doi.org/10.1145/3491102.3517668

[49] Allison Okamura, Mark Cutkosky, and Jack Dennerlein. 2001. Reality-based models for vibration feedback in virtual environments. *Mechatronics, IEEE/ASME Transactions on* 6 (Sept. 2001), 245–252. https://doi.org/10.1109/3516.951362

[50] A.M. Okamura, J.T. Dennerlein, and R.D. Howe. 1998. Vibration Feedback Models for Virtual Environments. In *Proceedings. 1998 IEEE International Conference on Robotics and Automation (Cat. No.98CH36146)*, Vol. 1. 674–679 vol.1. https://doi.org/10.1109/ROBOT.1998.677050

[51] Daniel S. Pamungkas and Wahyu Caesarendra. 2018. Overview Electrotactile Feedback for Enhancing Human Computer Interface. *Journal of Physics: Conference Series* 1007, 1 (April 2018), 012001. https://doi.org/10.1088/1742-6596/1007/1/012001

[52] Chaeyong Park, Jinhyuk Yoon, Seungjae Oh, and Seungmoon Choi. 2020. Augmenting Physical Buttons with Vibrotactile Feedback for Programmable Feels. In *Proceedings of the 33rd Annual ACM Symposium on User Interface Software and Technology (UIST '20)*. Association for Computing Machinery, New York, NY, USA, 924–937. https://doi.org/10.1145/3379337.3415837

[53] Giselle Prado and Carrie Kovarik. 2018. Cutting edge technology in dermatology: virtual reality and artificial intelligence. *Cutis* 101, 4 (April 2018), 236–237.

[54] Parinya Punpongsanon, Daisuke Iwai, and Kosuke Sato. 2015. SoftAR: Visually Manipulating Haptic Softness Perception in Spatial Augmented Reality. *IEEE Transactions on Visualization and Computer Graphics* 21, 11 (Nov. 2015), 1279–1288. https://doi.org/10.1109/TVCG.2015.2459792

[55] Andreas Pusch and Anatole Lécuyer. 2011. Pseudo-haptics: from the theoretical foundations to practical system design guidelines. In *Proceedings of the 13th international conference on multimodal interfaces (ICMI '11)*. Association for Computing Machinery, New York, NY, USA, 57–64. https://doi.org/10.1145/2070481.2070494

[56] Zhan Fan Quek, Samuel B. Schorr, Ilana Nisky, Allison M. Okamura, and William R. Provancher. 2014. Augmentation Of Stiffness Perception With a 1-Degree-of-Freedom Skin Stretch Device. *IEEE Transactions on Human-Machine Systems* 44, 6 (Dec. 2014), 731–742. https://doi.org/10.1109/THMS.2014.2348865

[57] Nihar Sabnis, Dennis Wittchen, Courtney N. Reed, Narjes Pourjafarian, Jürgen Steimle, and Paul Strohmeier. 2023. Haptic Servos: Self-Contained Vibrotactile Rendering System for Creating or Augmenting Material Experiences. In *Proceedings of the 2023 CHI Conference on Human Factors in Computing Systems (CHI '23)*. Association for Computing Machinery, New York, NY, USA, 1–17. https://doi.org/10.1145/3544548.3580716

[58] Steeven Villa Salazar, Claudio Pacchierotti, Xavier de Tinguy, Anderson Maciel, and Maud Marchal. 2020. Altering the Stiffness, Friction, and Shape Perception of Tangible Objects in Virtual Reality Using Wearable Haptics. *IEEE Transactions on Haptics* 13, 1 (Jan. 2020), 167–174. https://doi.org/10.1109/TOH.2020.2967389

[59] Katsunari Sato and Susumu Tachi. 2010. Design of electrotactile stimulation to represent distribution of force vectors. In *2010 IEEE Haptics Symposium*. 121–128. https://doi.org/10.1109/HAPTIC.2010.5444666

[60] Samuel B. Schorr and Allison M. Okamura. 2017. Fingertip Tactile Devices for Virtual Object Manipulation and Exploration. In *Proceedings of the 2017 CHI Conference on Human Factors in Computing Systems (CHI '17)*. Association for Computing Machinery, New York, NY, USA, 3115–3119. https://doi.org/10.1145/3025453.3025744

[61] Vivian Shen, Tucker Rae-Grant, Joe Mullenbach, Chris Harrison, and Craig Shultz. 2023. Fluid Reality: High-Resolution, Untethered Haptic Gloves using Electroosmotic Pump Arrays. In *Proceedings of the 36th Annual ACM Symposium on User Interface Software and Technology (UIST '23)*. Association for Computing Machinery, New York, NY, USA, 1–20. https://doi.org/10.1145/3586183.3606771

[62] Mike Sinclair, Eyal Ofek, Mar Gonzalez-Franco, and Christian Holz. 2019. CapstanCrunch: A Haptic VR Controller with User-supplied Force Feedback. In *Proceedings of the 32nd Annual ACM Symposium on User Interface Software and Technology (UIST '19)*. Association for Computing Machinery, New York, NY, USA, 815–829. https://doi.org/10.1145/3332165.3347891

[63] Smooth-On. 2023. Durometer Shore Hardness Scale. https://www.smooth-on.com/page/durometer-shore-hardness-scale/

[64] M. A. Srinivasan and R. H. LaMotte. 1995. Tactual discrimination of softness. *Journal of Neurophysiology* 73, 1 (Jan. 1995), 88–101. https://doi.org/10.1152/jn.1995.73.1.88

[65] A. A. Stanley, J. C. Gwilliam, and A. M. Okamura. 2013. Haptic jamming: A deformable geometry, variable stiffness tactile display using pneumatics and particle jamming. *2013 World Haptics Conference (WHC)* (April 2013), 25–30. https://doi.org/10.1109/WHC.2013.6548379

[66] S. S. Stevens. 1955. The Measurement of Loudness. *The Journal of the Acoustical Society of America* 27, 5 (1955), 815–829. https://doi.org/10.1121/1.1908048

[67] Paul Strohmeier, Sebastian Boring, and Kasper Hornbæk. 2018. From Pulse Trains to "Coloring with Vibrations": Motion Mappings for Mid-Air Haptic Textures. In *Proceedings of the 2018 CHI Conference on Human Factors in Computing Systems (CHI '18)*. Association for Computing Machinery, New York, NY, USA, 1–13. https://doi.org/10.1145/3173574.3173639

[68] Paul Strohmeier, Jesse Burstyn, Juan Pablo Carrascal, Vincent Levesque, and Roel Vertegaal. 2016. ReFlex: A Flexible Smartphone with Active Haptic Feedback for Bend Input. In *Proceedings of the TEI '16: Tenth International Conference on Tangible, Embedded, and Embodied Interaction (TEI '16)*. Association for Computing Machinery, New York, NY, USA, 185–192. https://doi.org/10.1145/2839462.2839494

[69] Paul Strohmeier, Seref Güngör, Luis Herres, Dennis Gudea, Bruno Fruchard, and Jürgen Steimle. 2020. bARefoot: Generating Virtual Materials using Motion Coupled Vibration in Shoes. In *Proceedings of the 33rd Annual ACM Symposium on User Interface Software and Technology (UIST '20)*. Association for Computing Machinery, New York, NY, USA, 579–593. https://doi.org/10.1145/3379337.3415828

[70] Yui Suga, Masahiro Takeuchi, Satoshi Tanaka, and Hiroyuki Kajimoto. 2023. Softness presentation by combining electro-tactile stimulation and force feedback. *Frontiers in Virtual Reality* 4 (2023). https://www.frontiersin.org/articles/10.3389/frvir.2023.1133146

[71] Taiki Takami, Taiga Saito, Takayuki Kameoka, Izumi Mizoguchi, and Hiroyuki Kajimoto. 2023. Pilot Study of Softness Presentation by Electro-Tactile Stimulation at the Edge of the Smartphone. *2023 IEEE World Haptics Conference (WHC)* (2023).

[72] Seiya Takei, Ryo Watanabe, Ryuta Okazaki, Taku Hachisu, and Hiroyuki Kajimoto. 2015. Presentation of Softness Using Film-Type Electro-Tactile Display and Pressure Distribution Measurement. In *Haptic Interaction: Perception, Devices and Applications*. 91–96. https://doi.org/10.1007/978-4-431-55690-9_17

[73] Yudai Tanaka, Alan Shen, Andy Kong, and Pedro Lopes. 2023. Full-hand Electro-Tactile Feedback without Obstructing Palmar Side of Hand. In *Proceedings of the 2023 CHI Conference on Human Factors in Computing Systems (CHI '23)*. Association for Computing Machinery, New York, NY, USA, 1–15. https://doi.org/10.1145/3544548.3581382

[74] Yujie Tao, Shan-Yuan Teng, and Pedro Lopes. 2021. Altering Perceived Softness of Real Rigid Objects by Restricting Fingerpad Deformation. In *The 34th Annual ACM Symposium on User Interface Software and Technology (UIST '21)*. Association for Computing Machinery, New York, NY, USA, 985–996. https://doi.org/10.1145/3472749.3474800

[75] Keigo Ushiyama and Pedro Lopes. 2023. FeetThrough: Electrotactile Foot Interface that Preserves Real-World Sensations. In *Proceedings of the 36th Annual ACM Symposium on User Interface Software and Technology (UIST '23)*. Association for Computing Machinery, New York, NY, USA, 1–11. https://doi.org/10.1145/3586183.3606808

[76] Anusha Withana, Daniel Groeger, and Jürgen Steimle. 2018. Tacttoo: A Thin and Feel-Through Tattoo for On-Skin Tactile Output. In *Proceedings of the 31st Annual ACM Symposium on User Interface Software and Technology (UIST '18)*. Association for Computing Machinery, New York, NY, USA, 365–378. https://doi.org/10.1145/3242587.3242645

[77] Dennis Wittchen, Valentin Martinez-Missir, Sina Mavali, Nihar Sabnis, Courtney N. Reed, and Paul Strohmeier. 2023. Designing Interactive Shoes for Tactile Augmented Reality. In *Proceedings of the Augmented Humans International Conference 2023 (AHs '23)*. Association for Computing Machinery, New York, NY, USA, 1–14. https://doi.org/10.1145/3582700.3582728

[78] Jacob O. Wobbrock, Leah Findlater, Darren Gergle, and James J. Higgins. 2011. The aligned rank transform for nonparametric factorial analyses using only anova procedures. In *Proceedings of the SIGCHI Conference on Human Factors in Computing Systems (CHI '11)*. Association for Computing Machinery, New York, NY, USA, 143–146. https://doi.org/10.1145/1978942.1978963

[79] Kuanming Yao, Jingkun Zhou, Qingyun Huang, Mengge Wu, Chun Ki Yiu, Jian Li, Xingcan Huang, Dengfeng Li, Jingyou Su, Senlin Hou, Yiming Liu, Ya Huang, Ziyan Tian, Jiyu Li, Hu Li, Rui Shi, Binbin Zhang, Jingyi Zhu, Tsz Hung Wong, Huiling Jia, Zhan Gao, Yuyu Gao, Yu Zhou, Wooyoung Park, Enming Song, Mengdi Han, Haixia Zhang, Junsheng Yu, Lidai Wang, Wen Jung Li, and Xinge Yu. 2022. Encoding of tactile information in hand via skin-integrated wireless haptic interface. *Nature Machine Intelligence* 4, 10 (Oct. 2022), 893–903. https://doi.org/10.1038/s42256-022-00543-y

[80] Seiedmuhammad Yazdian, Andrew J. Doxon, David E. Johnson, Hong Z. Tan, and William R. Provancher. 2014. Compliance display using a tilting-plate tactile feedback device. In *2014 IEEE Haptics Symposium (HAPTICS)*. 13–18. https://doi.org/10.1109/HAPTICS.2014.6775427

[81] Vibol Yem, Yasushi Ikei, and Hiroyuki Kajimoto. 2019. Shape and Stiffness Sensation Feedback with Electro-Tactile and Pseudo-Force Presentation When Grasping a Virtual Object. In *Haptic Interaction (Lecture Notes in Electrical Engineering)*, Hiroyuki Kajimoto, Dongjun Lee, Sang-Youn Kim, Masashi Konyo, and Ki-Uk Kyung (Eds.). Springer, Singapore, 327–330. https://doi.org/10.1007/978-981-13-3194-7_71

[82] Vibol Yem and Hiroyuki Kajimoto. 2017. Comparative Evaluation of Tactile Sensation by Electrical and Mechanical Stimulation. *IEEE Transactions on Haptics* 10, 1 (Jan. 2017), 130–134. https://doi.org/10.1109/TOH.2016.2605084

[83] Vibol Yem and Hiroyuki Kajimoto. 2018. Combination of Cathodic Electrical Stimulation and Mechanical Damped Sinusoidal Vibration to Express Tactile Softness in the Tapping Process. In *2018 IEEE Haptics Symposium (HAPTICS)*. 84–88. https://doi.org/10.1109/HAPTICS.2018.8357157

[84] Vibol Yem and Hiroyuki Kajimoto. 2018. A Fingertip Glove with Motor Rotational Acceleration Enables Stiffness Perception When Grasping a Virtual Object. In *Human Interface and the Management of Information. Interaction, Visualization, and Analytics (Lecture Notes in Computer Science)*, Sakae Yamamoto and Hirohiko Mori (Eds.). Springer International Publishing, Cham, 463–473. https://doi.org/10.1007/978-3-319-92043-6_39

[85] Vibol Yem, Kevin Vu, Yuki Kon, and Hiroyuki Kajimoto. 2018. Effect of Electrical Stimulation Haptic Feedback on Perceptions of Softness-Hardness and Stickiness While Touching a Virtual Object. In *2018 IEEE Conference on Virtual Reality and 3D User Interfaces (VR)*. 89–96. https://doi.org/10.1109/VR.2018.8446403